APPLIED GEOPHYSICS, Vol.9, No.3 (September 2012), P. 333 - 340, 7 Figures.
DOI: 10.1007/s11770-012-0346-0

Signal-purity-spectrum-based colored deconvolution*

Li Guo-Fa[1,2], Peng Geng-Xin[3], Yue Ying[4], Wang Wan-Li[1,2], and Cui Yong-Fu[3]

Abstract: Signal to noise ratio (SNR) and resolution are two important but contradictory characteristics used to evaluate the quality of seismic data. For relatively preserving SNR while enhancing resolution, the signal purity spectrum is introduced, estimated, and used to define the desired output amplitude spectrum after deconvolution. Since a real reflectivity series is blue rather than white, the effects of white reflectivity hypothesis on wavelets are experimentally analyzed and color compensation is applied after spectrum whitening. Experiments on real seismic data indicate that the cascade of the two processing stages can improve the ability of seismic data to delineate the geological details.
Keywords: signal purity spectrum, SNR spectrum, resolution, spectrum whitening, color compensation

Introduction

Due to the effect of high frequency noise, seismic data SNR decreases while increasing the resolution. Therefore, preserving SNR while enhancing resolution is a key technique for high resolution seismic data processing.

Kallweit and Wood (1982) discussed the limit and criterion of zero-phase wavelet resolution in the noise-free case but without involving the effect of noise on seismic resolution. Widess (1982) introduced the noise factor into the resolution definition and proposed the concept of signal purity but without involving the estimation of signal purity from seismic data. Li (1986, 2008) discussed the contradiction of resolution and SNR in depth and concluded that although deconvolution decreases the seismic data SNR, it doesn't change the SNR spectrum. Puyear and Castagna (2008) proposed spectral inversion. Velis (2008) introduced stochastic sparse-spike deconvolution. Compared with conventional deconvolution, both of the methods greatly improve seismic data resolution but noise factors aren't taken into account.

In addition to noise, another problem in conventional deconvolution is the white reflectivity hypothesis. Rosa and Ulrycht (1991) investigated a lot of log data and indicated that the spectrum of real reflectivity series is blue rather than white, i.e., the amplitude of low frequency components are relatively weaker than high frequency components. When the reflectivity of real seismic data deviates from white, the conventional

Manuscript received by the Editor May 17, 2012; revised manuscript received August 15, 2012.
*This research was financially supported by the National Natural Science Foundation of China (Grant No. 41174117) and PetroChina Innovation Foundation (Grant No. 2010D-5006-0301).
1. State Key Laboratory of Petroleum Resource and Prospecting (China University of Petroleum (Beijing)), Beijing 102249, China.
2. Key Laboratory of Geophysical Exploration of China National Petroleum Corporation, China University of Petroleum, Beijing 102249, China.
3. Tarim Oil Field, PetroChina, Korla 841000 China.
4. Dagang Oil Field, PetroChina, Tianjin 300280 China.

deconvolution methods, especially spectrum whitening and spectral modeling deconvolution, cannot play a full role in increasing resolution. Therefore, Zhao and Yu (1996) suggested that a blue filter should be applied for reflectivity color compensation. However, the effects of the white reflectivity hypothesis on wavelets after deconvolution have not been systematically analyzed and discussed.

After the discussion on the basic concept of the signal purity spectrum, we propose a method for the estimating the signal purity spectrum from seismic data in the f-x domain and use it to define the desired output amplitude spectrum after deconvolution. The SNR is preserved while enhancing resolution. Then, the effects of the white reflectivity hypothesis on wavelets are analyzed and color compensation is applied to further improve the resolution. The experiments on synthetic and real data indicate that the resolution and SNR are well balanced and the ability to describe the geological details is improved.

Signal purity and its spectrum

Suppose that a seismic record $x(t)$ consists of seismic signal $s(t)$ and noise $n(t)$

$$x(t)=s(t)+n(t), \tag{1}$$

The equation can also be expressed in frequency domain as

$$X(f)=S(f)+N(f), \tag{2}$$

The signal purity can be define as

$$P=\frac{\int s^2(t)dt}{\int s^2(t)dt+\int n^2(t)dt}=\frac{\int S^2(f)df}{\int S^2(f)df+\int N^2(f)df}=\frac{1}{1+1/R}, \tag{3}$$

where R is SNR and it is defined as

$$R=\frac{\int s^2(t)dt}{\int n^2(t)dt}=\frac{\int S^2(f)df}{\int N^2(f)df}, \tag{4}$$

The signal purity spectrum is referred as signal purity for each frequency component

$$p(f)=\frac{S^2(f)}{S^2(f)+N^2(f)}, \tag{5}$$

For convenience and no loss of generality, the signal purity spectrum is defined here as

$$p(f)=\frac{|S(f)|}{|S(f)|+|N(f)|}=\frac{1}{1+1/r(f)}, \tag{6}$$

where $r(f)$ is defined as SNR spectrum.

The seismic record after deconvolution is denoted in the frequency domain as

$$Y(f)=X(f)H(f), \tag{7}$$

where $H(f)$ is the deconvolution operator in the frequency domain and the signal purity spectrum after deconvolution is

$$p_y(f)=\frac{|H(f)||S(f)|}{|H(f)|\left[|S(f)|+|N(f)|\right]}=\frac{1}{1+1/r(f)}=p(f), \tag{8}$$

Equation (8) indicates that deconvolution cannot change the signal purity spectrum of a seismic record since signal and noise for a given frequency are scaled by the same operator, although the SNR of the whole record may decrease.

Figure 1 shows a seismic signal, noise, and seismic record, as well as their amplitude spectra before and after deconvolution. Figure 1 (a) to (f) are sequentially the seismic signal, noise, and seismic record before and after deconvolution and Figure 1 (g) to (l) are the amplitude spectra of the seismic signal, noise, and seismic record before and after deconvolution. The SNR and signal purity before deconvolution are 5.278 and 0.841, respectively. They are decreased to 1.401 and 0.584 after deconvolution. We can explain intuitively from the amplitude spectra shown in Figure 1. The high frequency components above 90 Hz contribute more proportion to the complete seismic record after deconvolution than before. However, the high frequency components are mostly occupied by noise.

Figure 2 shows the signal purity spectra before and after deconvolution. It is clear that although signal purity of the whole seismic record is decreased after deconvolution, its spectrum has not been changed by deconvolution.

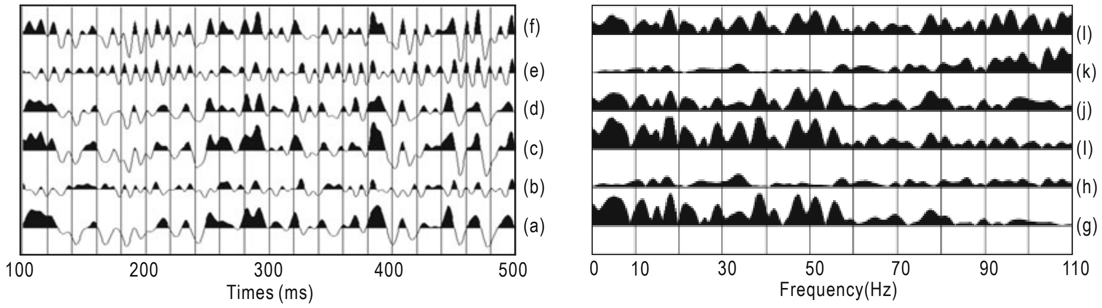

Fig.1 Deconvolution decreases SNR while increasing resolution.
(a) - (f) are sequentially signal, noise, and seismic record before and after deconvolution and (g) - (l) are sequentially the spectra of the signal, noise, and seismic record before and after deconvolution.

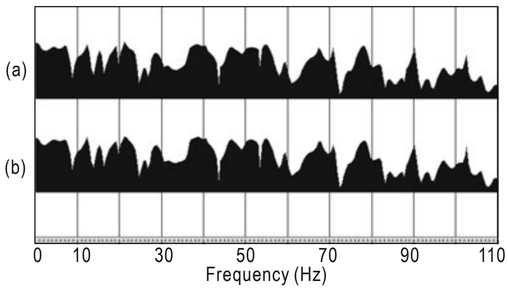

Fig.2 Signal purity spectra before (a) and after (b) deconvolution.

Estimation of signal purity spectrum from seismic records

Canales (1984) presented an *f-x* domain random noise attenuation method. The basic idea of the method is that, for a given frequency, the predictable part of the seismic data, which can be thought as signals, can be estimated by seismic data convolved in spatial directions with a spatial prediction filtering operator which can be found by minimizing the prediction error. Soubaras (1994) improved the method in estimated noise accuracy by projection filtering. It is not difficult to extend the method from noise attenuation to signal purity spectrum estimation.

Suppose there are N seismic records $X_i(f)$ in the frequency domain,

$$X_i(f) = S_i(f) + N_i(f), \quad i = 1, 2, \cdots, N-1, N. \tag{9}$$

For a given frequency f_0, signal $S_i(f_0)$ is laterally predictable by

$$S_i(f_0) = \sum_{j=1}^{m} Q_j(f_0) S_{i-j}(f_0), \tag{10}$$

where $Q_i(f_0)$ is the prediction operator with length m.

Supposing noise is laterally random, then signals can be predicted from seismic records with noise by

$$S_i(f_0) = \sum_{j=1}^{m} Q_j(f_0) X_{i-j}(f_0), \tag{11}$$

where $Q_i(f_0)$ can be obtained by minimizing the prediction error $E(f_0)$:

$$E(f_0) = \sum_i \left\| \sum_{j=1}^{m} Q_j(f_0) X_{i-j}(f_0) - X_i(f_0) \right\|^2, \tag{12}$$

The signal $s_i(f_0)$ can be abstracted from seismic record $X_i(f_0)$ by equation (11) and then signal purity at frequency f_0 can be estimated by equation (6).

Signal-purity-spectrum-based deconvolution

The core of linear deconvolution is compression of the wavelet duration time by broadening the frequency band (Li, et al., 2008, 2010a). Two problems are involved in the process, one is how to estimate the input wavelet from seismic records and the other is how to define the desired output wavelet. Since it is difficult to directly estimate the wavelet from seismic records, the wavelet is often assumed to be minimum-phase or zero-phase because only the amplitude spectrum or auto-correlation is estimated from the seismic records. On this basis, the input wavelet amplitude spectrum is modulated towards the desired output spectrum for increasing resolution. There are many literatures involving the wavelet amplitude spectrum estimation (Porsani and Ursin, 2000; Li, et al., 2005) so we will not discuss this topic further in this paper. We will focus on how to define the desired output amplitude spectrum.

For noise-free data, broadening the desired output wavelet spectrum increases the seismic resolution after deconvolution. However, seismic signals are much feebler than noise at high frequencies because of absorption (Li, et al., 2010b). The amplification of high frequency components increase the resolution, meanwhile inevitably decreasing the SNR. Therefore, how to relatively preserve SNR while increasing resolution is an important concern in seismic data processing.

The seismic data spectral distribution after deconvolution determines the SNR and resolution. Therefore, the optimum output spectrum with balanced SNR and resolution should be found to improve the overall quality of seismic data to the maximum extent. The signal purity spectrum representing the signal purity at each frequency remains unchanged after deconvolution, therefore, it can be used as an optimum output spectrum. If the desired output spectrum after deconvolution is defined by the signal purity spectrum, SNR and resolution balance can be achieved.

Figure 3 shows the role of the signal purity spectrum. Figure 3a is synthetic seismograms with random noise. The wavelet is the Ormsby wavelet, whose spectrum is a trapezoid defined by the four frequencies 2, 8, 30, and 95 Hz. The four frequencies represent the 0% and 100% points of the low-cut ramp and 100% and 0% points of the high-cut ramp. There are nine reflection events in the model, with the fourth, fifth, eighth, and ninth are less resolvable. Figure 3b is the average signal purity spectrum. The purity above 90 Hz is less than 0.2. By defining the desired output spectrum as a 2, 8, 80, and 100 Hz trapezoid, Figure 3c shows the deconvolution result. The resolution is improved and the fourth, fifth, eighth, and ninth events are resolvable but the SNR is significantly decreased. For better preservation of seismic SNR, the desired output amplitude spectrum is defined by the signal purity spectrum and the deconvolution result is displayed in Figure 3d. The SNR is preserved while the resolution is enhanced.

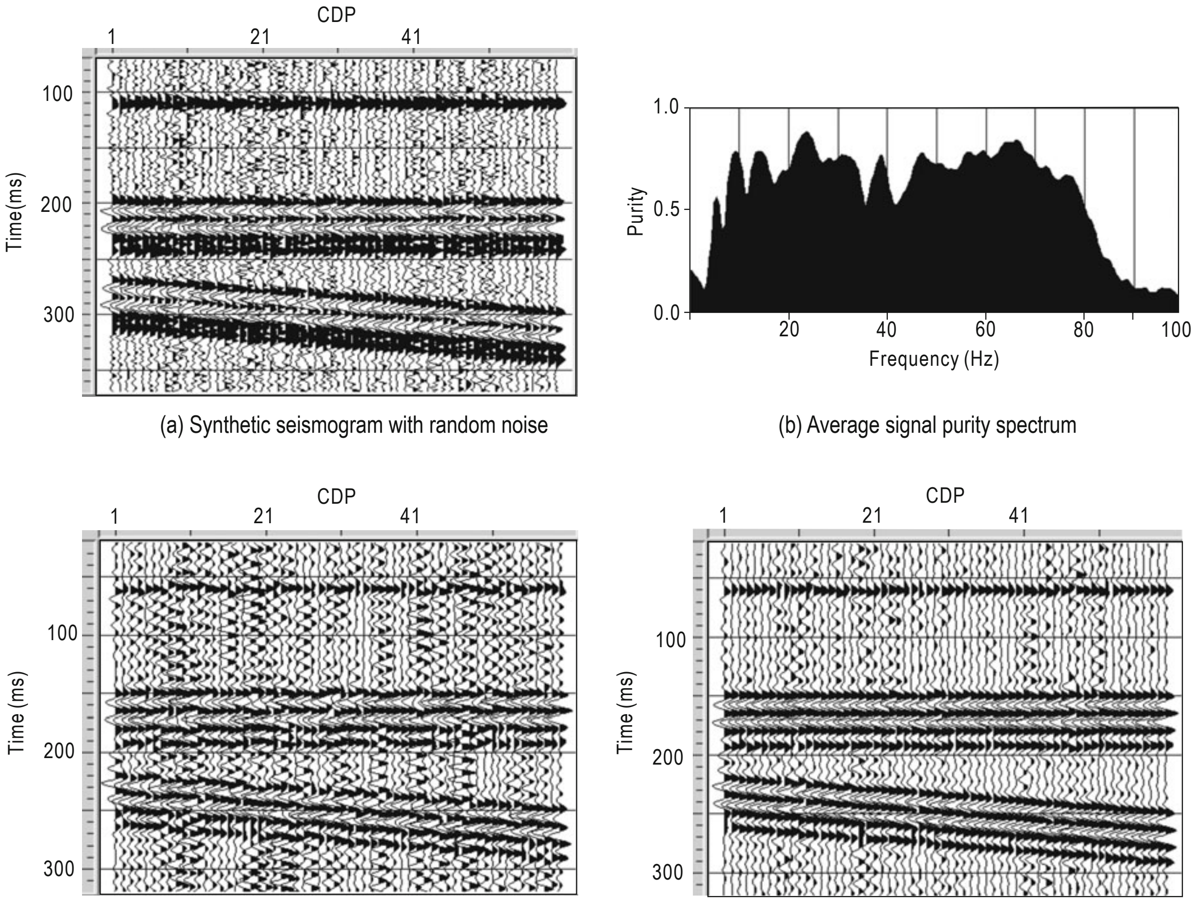

(a) Synthetic seismogram with random noise

(b) Average signal purity spectrum

(c) Deconvolution output for a 2-8-80-100 Hz trapezoidal spectrum

(d) Deconvolution output based on the signal purity spectrum

Fig.3 Deconvolution with the signal purity spectrum.

Effect of white reflectivity hypothesis on the wavelet

Deconvolution methods, such as spike and prediction deconvolution, spectrum whitening, and spectral modeling, imply the white reflectivity hypothesis. Analysis of log data indicates that real reflectivity is blue rather than white, i.e., the low frequency components are relatively weaker than high frequency components (Walden and Hosken, 1985; Rosa and Ulrycht, 1991). The reflectivity spectrum can be modeled as (Rosa and Ulrycht, 1991):

$$\left|\xi\left(f\right)\right| = \left|2\sin\left(\pi f \Delta t\right)e^{-i(\pi/2-\pi f\Delta t)}\right|^{b}, \tag{13}$$

where b is a constant larger than zero.

In practice, blue compensation can be represented as an ARMA process (Walden, 1988; Zhao and Yu, 1996). The Z-transformation of the color compensation operator can be expressed as

$$c\left(z\right) = \frac{1-\theta z}{1-\varphi z}, \tag{14}$$

where θ and φ can be estimated from log data and $|\theta| < 1$, $|\varphi| < 1$.

The color compensation process can be represented in Z-transformation as

$$y\left(z\right) = x\left(z\right)\frac{1-\theta z}{1-\varphi z}, \tag{15}$$

where $x(z)$ is the input signal Z-transformation and $y(z)$ is the output signal Z-transformation after color compensation.

The potential effect of the white reflectivity hypothesis on wavelets after deconvolution will be discussed below.

For a seismic record $x(t)$, its reflectivity $\xi(t)$ is blue and its wavelet $w(t)$ is band-limited with a rectangular spectrum. Figures 4a, 4b, and 4c are the spectra of the reflectivity, wavelet, and seismic record before spectrum whitening. The seismic record spectrum is modulated to white after spectrum whitening with the wavelet spectrum changed to

$$\left|w'\left(f\right)\right| = \frac{1}{\left|\xi\left(f\right)\right|}, \tag{16}$$

Figures 4d, 4e, and 4f schematically show the spectra of the reflectivity, wavelet, and seismic record, after spectrum whitening. The wavelet spectrum is modified into red, i.e., with strong low frequency amplitude and weak high frequency amplitude. As a result the output wavelet has less perfect ability to resolve thin strata.

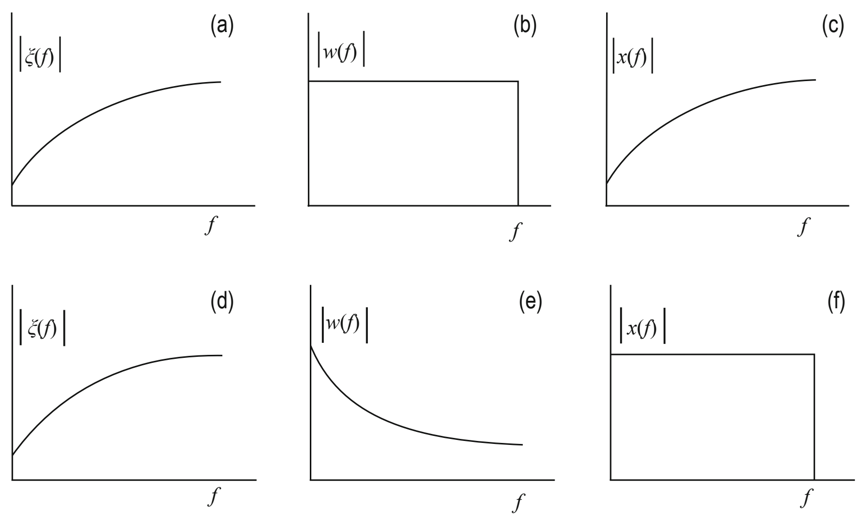

Fig.4 Wavelet amplitude spectra before and after deconvolution in the condition of blue reflectivity.
(a) to (c) are the spectra of reflectivity, wavelet, and seismic record, respectively, before deconvolution and (d) to (f) are the spectra of reflectivity, wavelet, and seismic record after deconvolution.

The effect of the white reflectivity hypothesis on the wavelet after spectrum whitening is well displayed using a synthetic seismogram in Figure 5. Figure 5a is the synthetic seismogram with blue reflectivity. Figure 5b is the result of spectrum whitening with the desired output spectrum defined as trapezoid with 4 to 10 Hz low-cut ramp and 70 to 80 Hz high-cut ramp. Except for the improved resolution, no visual anomaly is found in Figure 5b.

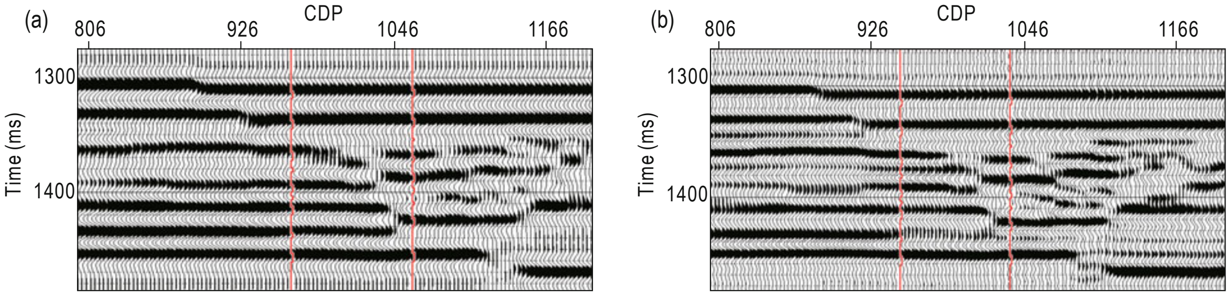

Fig.5 Synthetic seismogram with blue reflectivity before (a) and after (b) spectrum whitening.

We extract the wavelet after spectrum whitening with the help of one model reflectivity series to investigate the influence of the white reflectivity hypothesis on the wavelet. The extracted wavelet and its spectrum are displayed in Figures 6a and 6b. As expected, since the real reflectivity is blue rather than white, the spectrum whitening deconvolution adjusts the seismic data spectrum to white at the expense of making the wavelet red.

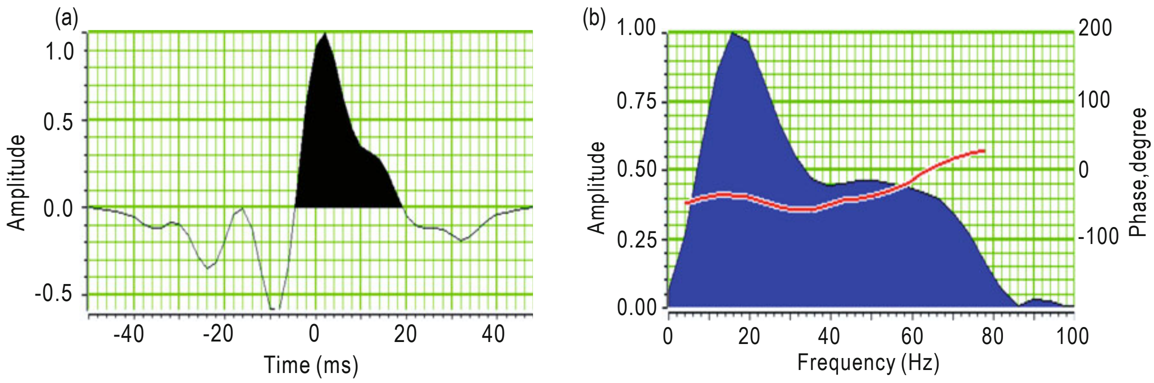

Fig.6 The extracted wavelet (a) and its spectra (b) from the data after spectrum whitening.

Real data example

We use real seismic data from Dagang Oilfield, China, as an example to test the proposed deconvolution method. Figure 7a is a seismic section after pre-stack time migration, where the red trace is a synthetic seismogram at well X1 with a zero-phase wavelet of 5-10-60-75 Hz trapezoid spectrum. Since the seismic data lacks high frequencies, the resolution is not high enough to resolve the target details near 2200 ms indicated by a blue circle. Figure 7b is the average signal purity spectrum. Figure 7c is the result of spectrum whitening using the average signal purity spectrum as desired output. The resolution is greatly increased while, the SNR is decreased but not too much. The strong reflection just below 2200 ms is separated into two events, one with strong amplitude and the other with weak amplitude.

Next, we investigate the reflectivity color spectrum calculated from acoustic log data of well X1 to make clear whether the seismic data in Figure 7c should be color-compensated. Figure 7d is the reflectivity amplitude spectrum of well X1. As indicated by the black dash curve, the amplitude below 50 Hz increases with frequency increasing and the spectrum becomes gradually flat above 50 Hz. It is the typical blue spectrum characteristic. Therefore, it is necessary to compensate the seismic data color after whitening in Figure 7c. Figure 7e is the result of color compensation. Compared with Figure 7c, the resolution is further improved. For the two reflections right below 2200 ms in Figure 7e, their amplitudes become almost the same from one strong and one weak amplitude before color compensation. It is more similar to the reflection characteristic of the synthetic seismogram. As a result, color compensation not only improves the resolution but also makes the reflection characteristics more reliable. The latter is more valuable in thin reservoir prediction.

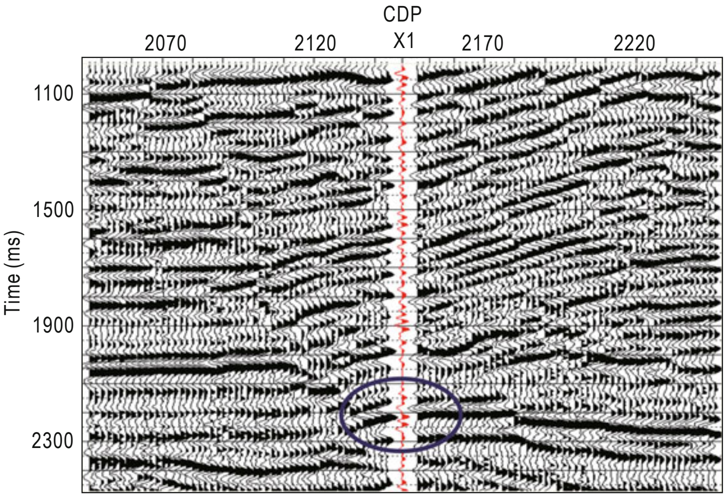

(a) Prestack time migration section across well X1, the red trace is a synthetic seismogram at well X1

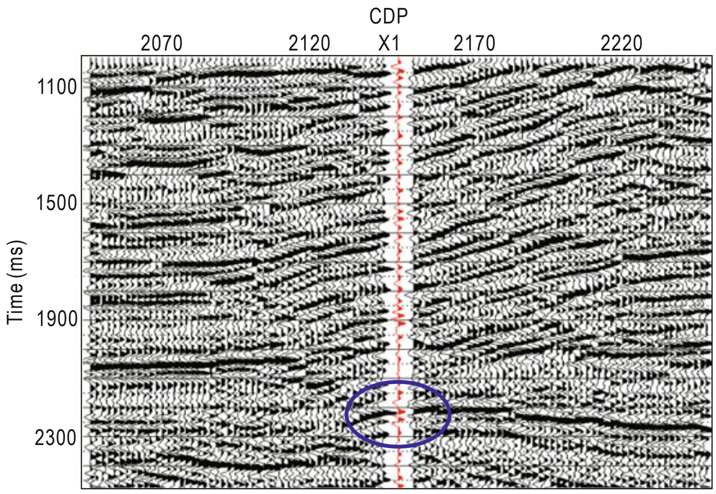

(c) Spectrum whitened section based on signal purity spectrum

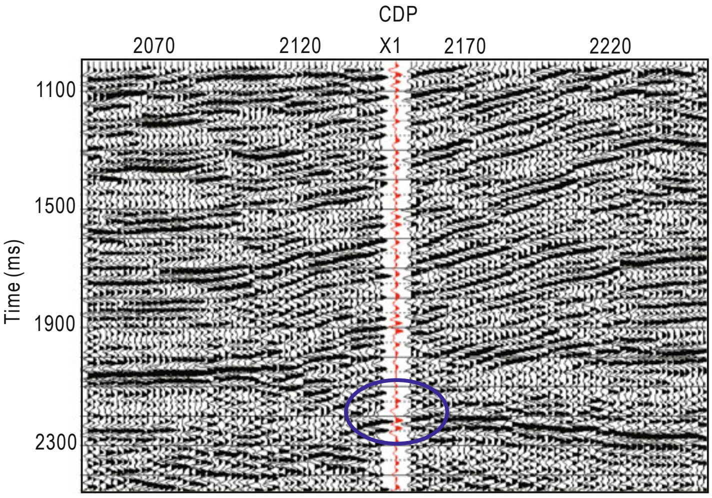

(e) The section after color compensation for section (c)

Fig.7 A real data example from Dagang Oilfield.

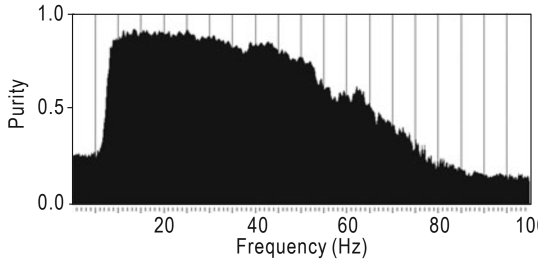

(b) Average signal purity spectrum

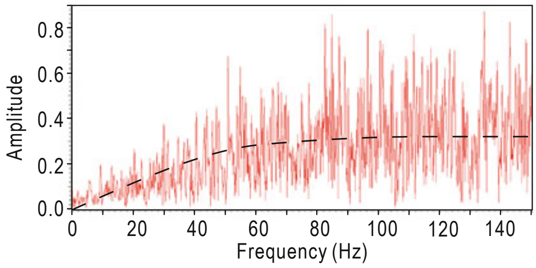

(d) The amplitude spectrum of the well X1 reflectivity

Conclusions

(1) Although deconvolution decreases the SNR of noisy seismic data, it does not change the SNR spectrum and signal purity spectrum.

(2) The desired output spectrum after deconvolution can be well defined on the basis of the signal purity spectrum. In this way, SNR can be relatively preserved while increasing resolution and the optimum balance between SNR and resolution can be achieved.

(3) When reflectivity is blue, the spectrum whitening deconvolution, based on the white reflectivity hypothesis, makes the wavelet spectrum red.

(4) Color compensation not only improves the resolution of seismic data but also makes the reflection characteristics more reliable. The latter is more valuable in thin reservoir prediction using the reflections characteristics.

References

Canales L. L., 1984, Random noise reduction: 54th Ann. Internat. Mtg., Soc. Explor. Geophys., Expanded Abstracts, 525 – 527.

Kallweit, R. S., and Wood, L. C., 1982, The limit of resolution of zero-phase wavelets: Geophysics, **47**(7), 1035 – 1046.

Li, G. F., Mou, Y. G., and Wang, P., 2005, A interactive technique for seismic wavelet extraction: Journal of the University of Petroleum (in Chinese), **29**(5), 33 – 36.

Li, G. F., Xiong, J. L., et al., 2008, Seismic reflection characteristics of fluvial sand and shale interbedded layers: Applied Geophysics, **5**(3), 219 – 229.

Li, G. F., Cao, M. Q., et al., 2010a, Modeling of the signature of air gun in marine seismic exploration considering the effects of multiple practical physics: Applied Geophysics, **7**(2), 158 – 165.

Li, G. F., Cao, M. Q., and Zhou, H., 2010b, Effects of near-surface absorption on the reflection characteristics of continental interbedded strata: the Dagang Oilfield as an example: ACTA GEOLOGICA SINICA, **84**(5), 1306 – 1314.

Li, Q. Z., 1986, The evaluation of filtering and deconvolution effects by S/N spectrum analysis—A study of S/N ratio and resolution in frequency domain: Oil Geophysical Prospecting(in Chinese), **21**(6), 575 – 601.

Li, Q. Z., 2008, Relationship between resolution of seismic exploration and spectrum of S/N ratio: Oil Geophysical Prospecting(in Chinese), **43**(2), 244 – 245.

Porsani, M. J., and Ursin, B., 2000, Mixed-phase deconvolution and wavlet estimation: The Leading Edge, **19**, 76 – 79.

Puryear, C. I., and Castagna, J. P., 2008, Layer-thickness determination and stratigraphic interpretation using spectral inversion: Theory and application: Geophysics, **73**(2), R37 – R38.

Rosa, A. L. R., and Ulrycht, T. J., 1991, Processing via spectral modeling: Geophysics, **56**(8), 1244 – 1251.

Soubaras, R., 1994, Signal-preserving random noise attenuation by the *f-x* projection: 64th Ann. Internat. Mtg., Soc. Expl. Geophys., Expanded Abstracts, 1576 – 1579.

Velis, D. R., 2008, Stochastic sparse-spike deconvolution: Geophysics, **73**(1), R1 – R9.

Walden, A. T., and Hosken, J. W. J., 1985, An investigation of the spectral properties of primary reflection coefficients: Geophysical Prospecting, **33**, 400 – 435.

Widess, M. B., 1982, Quantifying resolving power of seismic system: Geophysics, **47**(8), 1160 – 1173.

Zhao, B., and Yu, S. P., 1996, Spectral-modeled deconvolution and its application: Oil Geophysical Prospecting (in Chinese), **31**(1), 101 – 113.

Li Guo-Fa received a B. S. in Geophysics from Changchun Geology College in 1987, PhD from China University of Petroleum (Beijing) in 2002, and Postdoctoral from China University of Mining (Beijing) in 2005. He currently works in China University of Petroleum (Beijing) as an Associate Professor. His research work mainly focuses on high resolution seismic data processing and complex structure seismic imaging.